

From Alkynols to Alkynol Complexes. A Molecular Assembly Study

Dario Braga*[†] and Fabrizia Grepioni

*Dipartimento di Chimica G. Ciamician, Università di Bologna, Via Selmi 2,
40126 Bologna, Italy*

Dirk Walther,* Kirstin Heubach, Andreas Schmidt, Wolfgang Imhof,
Helmar Görls, and Thomas Klettke

*Institut für Anorganische und Analytische Chemie der Universität, A.-Bebel-Strasse 2,
07743 Jena, Germany*

Received April 18, 1997[Ⓢ]

The solid state supramolecular assembly of prop-2-yn-1-ol and alkynediol transition metal complexes of Pt and Ni has been examined in light of the intermolecular interactions and hydrogen-bonding patterns established by alkyne monoalcohols and diols in the solid state. The analysis has been based on the crystal structure determination of the alcohols 1,1-dimethyl-3-*tert*-butylprop-2-yn-1-ol (**1**), *tert*-butylbis(ethyl)prop-2-yn-1-ol (**2**), *tert*-butylcyclohexylprop-2-yn-1-ol (**3**), and tetramethylalkynediol (**4**), as well as of the complexes bis(*t*-butylcyclohexylprop-2-yn-1-ol)M(0) (M = Pt (**6a**) and Ni (**6b**)) and bis(*t*-butylcyclopentylprop-2-yn-1-ol)Pt(0) (**7**), integrated with the data available in the Cambridge Structural Database. It has been shown that the most common hydrogen-bond pattern is that based on a tetramer of –OH groups forming a square, a rhombus, or an open butterfly, irrespective of the molecular complexity. Larger ring systems or chains are established depending on the steric bulk of the substituents on the prop-2-yn-1-ol. Intermolecular and intramolecular hydrogen bond distances have been shown to depend on the type of alcohols, differences having largely a steric origin. The change in the Raman/IR stretching frequency of the C≡C bond upon coordination of alkynediols to the metal centers has been examined for the nickel compounds and shown to provide a diagnostic tool for recognition of hydrogen-bond formation and typology.

Introduction

Molecular crystal engineering is the planning of a crystal structure from its building blocks.¹ The building blocks are molecules or ions chosen on the basis of their size, shape, and extramolecular bonding capacity. The engineering of molecular crystals as well as the construction of supramolecular aggregates are both concerned with intermolecular interactions, hence crystal engineering and supramolecular chemistry are conceptually connected.²

The groups of Bologna and Jena have approached inter- and intramolecular interactions in organometallic solids in the context of crystal engineering and supramolecular synthesis. A systematic investigation of the way neutral and charged organometallic molecules self-recognize and self-assemble in the solid state has been carried out in Bologna.³ The objective was (and is) that of achieving sufficient basic knowledge to be able to *choose* intermolecular interactions to project the

synthesis of novel crystalline materials on the basis of shape, size, and structural functionality. The design of supramolecular aggregates between the paramagnetic cations [(η⁶-arene)₂Cr]⁺ (arene = benzene and toluene) and 1,3-cyclohexanedione (CHD) with the participation of water in the intermolecular hydrogen-bonding patterns has led to the aggregation of the dione in superanions and/or in extended hydrated aggregates which are based on strong hydrogen bonds, whereas the interaction between organic aggregates and the organometallic complexes is based on weak C–H...O hydrogen bonds reinforced by the different polarity.⁴ At Jena inter- and intramolecular interactions, in particular hydrogen bonds between –OH groups, have been exploited to isolate zerovalent homoleptic compounds of the composition (alkyne)₂Ni and (alkyne)₄Ni₃, thanks to the stabilization afforded in the solid state by hydrogen bonds between alkynediol and prop-2-yn-1-ols groups. These complexes are of great interest as starting materials for organometallic reactions and for their utilization in catalytic processes.⁵

In this paper, we report the results of a comparative study of the intermolecular architecture in crystalline prop-2-yn-1-ol and alkynediol transition metal complexes of Pt and Ni and in the crystal structures of organic alkyne monoalcohols and alkyne diols. The

[†] E-mail: dbraga@ciam.unibo.it.

[Ⓢ] Abstract published in *Advance ACS Abstracts*, September 1, 1997.
(1) (a) Schmidt, G. M. J. *Pure Appl. Chem.* **1971**, *27*, 647. (b) Sharma, C. V. K.; Desiraju, G. R. In *Perspective in Supramolecular Chemistry. The Crystal as a Supramolecular Entity*; Desiraju, G. D., Ed.; Wiley: New York, 1996. (c) Etter M. C. *Acc. Chem. Res.* **1990**, *23*, 120. (d) Braga, D.; Grepioni, F. *Acc. Chem. Res.* **1994**, *27*, 51.

(2) (a) Lehn, J.-M.; Mascal, M.; Fisher, J. *J. Chem. Soc., Chem. Commun.* **1990**, 479. (b) Etter, M. C. *J. Am. Chem. Soc.* **1982**, *104*, 1095.

(3) Braga, D.; Grepioni, F. *J. Chem. Soc., Chem. Commun.* **1996**, 571.

(4) Braga, D.; Grepioni, F.; Byrne, J. J.; Wolf, A. *J. Chem. Soc., Chem. Commun.* **1995**, 1023. Braga, D.; Costa, A. L.; Grepioni, F.; Scaccianoce, L.; Tagliavini, E. *Organometallics* **1996**, *15*, 1084.

primary objective of this study is to investigate the transferability of hydrogen-bond patterns from those established by the "free" alcohols to those established by the corresponding metal-coordinated alkyne alcohols. This is instrumental to crystal engineering in that we can expect to be able to choose ligands for metal complexation as a function of the desired pattern of intermolecular interactions.

Complementary hydrogen bonds have also been employed by Mingos *et al.* to co-crystallize bifunctional transition metal complexes with organic bases in order to construct solid state sheet and tape structures.⁶

The hydrogen bond is the key interaction in crystal engineering. Some of us have undertaken a systematic study of the hydrogen bonds in organometallic crystals. Hydrogen bonds formed by strong donor/acceptor groups such as $-\text{COOH}$ and $-\text{OH}$ systems,^{7a} as well as by primary $-\text{CONH}_2$ and secondary amido $-\text{CONHR}$ groups belonging to metal-coordinated ligands, have been investigated and compared with those formed by the corresponding organic molecules in their crystals.^{7b} Hydrogen bonds of the C–H...O type have also been studied. These interactions are pervasive in crystalline organometallic transition metal complexes and clusters where C–H groups (mainly in sp^2 - and sp -hybridized systems) and the CO base are abundant.⁸ The amphoteric behavior of the M–H group (M = transition metal atom) in the formation of hydrogen bonds with suitable donor or acceptor groups has also been investigated.⁹ The hydrogen bonds formed by alcohols have been less studied.¹⁰ Recently, the crystal packing of monoalcohols has been investigated with a focus on the occurrence of high-symmetry space groups.¹¹

The crystal structures of organic prop-2-yn-1-ols and alkyne diols discussed in this paper have been either determined by low-temperature single-crystal X-ray diffraction experiments (see below) or obtained from Cambridge Structural Database¹² (CSD) searches. Similarly, some novel Pt and Ni prop-2-yn-1-ol complexes have been characterized and the molecular organization compared with that observed in previously determined structures. On the basis of this information, hydrogen-bond patterns have been compared in terms of geometry and strength.

Finally, the Raman stretching frequency of the $\text{C}\equiv\text{C}$ bond upon coordination of prop-2-yn-1-ols and alkyne diols to the metal centers has been correlated with the

formation of intra- or intermolecular bonds, thus affording a diagnostic tool for the recognition of hydrogen-bond formation and typology.

Experimental Section

Synthesis and Chemical Characterization. General Considerations. All operations were carried out under argon using standard Schlenk and vacuum techniques. Solvents for the syntheses and the NMR measurements were dried and distilled from sodium biphenyl ketyl. The alcohols 1,1-dimethyl-3-*tert*-butylprop-2-yn-1-ol (**1**), 1,1-diethyl-3-*tert*-butylprop-2-yn-1-ol (**2**), 1-cyclohexyl-3-*tert*-butylprop-2-yn-1-ol (**3**) and 1-cyclopentyl-3-*tert*-butylprop-2-yn-1-ol (**5**) were prepared from *tert*-butylacetylene (Aldrich) by reaction with butyllithium and the appropriate ketone. 1,1,4,4-Tetramethylbut-2-yne-1,4-diol (**4**) was obtained from Lancaster. The properties of the different alkynes are reported, see the following listed Beilstein Registry Numbers: 1 745 820 (**1**), 1 904 249 (**2**), 5 499 974 (**3**), 1 765 925 (**4**), 5 498 287 (**5**). The complexes (cdt)-Ni and (cod)₂Pt were prepared as described in the literature.¹³

A Bruker AC 200 spectrometer was used for the 100 MHz ¹H and 50.3 MHz ¹³C NMR spectra. Infrared spectra: Perkin-Elmer FT IR system, KBr plates. Mass spectra: Finnigan MAT SSQ 710 mass spectrometer. Raman spectra: JASCO-1100.

Preparation of Organometallic Compounds. Bis(1-cyclohexyl-3-*tert*-butylprop-2-yn-1-ol)Pt(0) (6a**).** Pt(cod)₂ (0.38 mmol, 0.156 g) and 1-cyclohexyl-3-*tert*-butylprop-2-yn-1-ol (0.76 mmol, 0.136 g) were mixed in 40 mL of pentane at -30°C . The solution was allowed to reach room temperature. It was stirred at room temperature for 0.5 h, was then filtered and concentrated to 3 mL. At -78°C , **6a** precipitated. The isolated white powder was washed with pentane at -70°C and dried in vacuum. Single crystals were obtained from pentane at -25°C . Yield: 0.205 mmol (0.11 g); 54.1%. Anal. Calcd for C₂₄H₄₀O₂Pt (555.66): C, 51.88; H, 7.26. Found: C, 51.55; H, 7.22. IR (Nujol): $\tilde{\nu} = 1903$ (s, $\text{C}\equiv\text{C}$), 3349 (s, OH) cm^{-1} . ¹H NMR (THF-*d*₈, 25°C , 200 MHz): δ 1.25 (s, CH₃, 18 H), 1.59–1.80 (m, CH₂, 20 H), 3.58 (s, OH, 2 H). ¹³C NMR (THF-*d*₈, 25°C , 50.3 MHz): δ 23.4, 26.5, 40.8 (CH₂), 29.8 (CMe₃), 31.9 (CH₃), 66.6 (C–OH), 128.1, 131.7 (C \equiv C). MS (EI): m/e 555 (M⁺; 24), the isotopic pattern corresponds well to the simulated one 537 (M⁺ – H₂O, 3), 355 (M⁺ – prop-2-yn-1-ol – 20, 66), 41 (100%). Mp: 91°C . (dec at 289°C).

Bis(1-cyclohexyl-3-*tert*-butylprop-2-yn-1-ol)Ni(0) (6b**).** Ni(cdt) (0.97 mmol, 0.21 g) and 1-cyclohexyl-3-*tert*-butylprop-2-yn-1-ol (1.94 mmol, 0.349 g) were mixed in 10 mL of pentane at -40°C . The solution was allowed to warm to room temperature. After filtration, the solution was concentrated to 5 mL. Compound **6b** precipitated as yellow crystals at -25°C . Single crystals were obtained from pentane or ether at -25°C . Yield: 0.46 mmol (0.193 g); 47.4%. Anal. Calcd for C₂₄H₄₀O₂Ni (419.27): C, 68.75; H, 9.62; Ni, 14.00. Found: C, 68.30; H, 9.58; Ni, 14.12. IR (Nujol): $\tilde{\nu} = 1911$ (s, $\text{C}\equiv\text{C}$), 3334 (s, OH) cm^{-1} . ¹H NMR (THF-*d*₈, 25°C , 200 MHz): δ 1.29 (s, CH₃, 18 H), 1.40–1.82 (m, CH₂, OH, 22 H). ¹³C NMR (DMF-*d*₇, 25°C , 50.3 MHz): δ 23.8, 26.5 (CH₂), 31.5 (CMe₃), 32.0, 41.2 (CH₂), 69.2 (C–OH), 132.7, 137.2 (C \equiv C). (dec at 122°C).

Bis(1-cyclopentyl-3-*tert*-butylprop-2-yn-1-ol)Pt(0) (7**).** Pt(cod)₂ (0.41 mmol, 0.167 g) was suspended in 40 mL of pentane at -30°C . A solution of 1-cyclopentyl-3-*tert*-butylprop-2-yn-1-ol (0.81 mmol, 0.135 mg) in 20 mL of pentane was then added. After the solution was warmed to room temperature, it was stirred for 2 h. Then it was concentrated to 2 mL. At -78°C , **7** precipitated. The precipitate was isolated, washed with cold pentane, and dried in vacuum. Single crystals were obtained from the mother solution at room temperature. Yield: 0.175 mmol (0.92 g); 42.9%. Anal. Calcd

(13) (a) Herberich, G. E.; Hessner, B. *Z. Naturforsch.* **1979**, *34b*, 638. (b) Bogdanovic, B.; Kröner, M.; Wilke, G. *Justus Liebig's Ann. Chem.* **1966**, *699*, 19.

(5) (a) Walther, D.; Klettke, T.; Schmidt, A.; Görls, H.; Imhof, W. *Organometallics* **1996**, *15*, 2314. (b) Walther, D.; Schmidt, A.; Klettke, T.; Imhof, W.; Görls, H. *Angew. Chem.* **1994**, *106*, 1421; *Angew. Chem., Int. Ed. Engl.* **1994**, *33*, 1373. (c) Walther, D.; Klettke, T.; Görls, H. *Angew. Chem.* **1995**, *107*, 2022; *Angew. Chem., Int. Ed. Engl.* **1995**, *34*, 1860. (d) Klettke, T.; Walther, D.; Schmidt, A.; Görls, H.; Imhof, W.; Günther, W. *Chem. Ber.* **1996**, *129*, 1457. (e) Walther, D.; Klettke, T.; Imhof, W.; Görls, H. *Z. Anorg. Allg. Chem.* **1996**, *622*, 1134. (f) Dubey, R. J. *Acta Crystallogr., Sect. B* **1975**, *31*, 1860.

(6) Burrows, A. D.; Chan, C.-W.; Chowdry, M. M.; McGrady, J. E.; Mingos, D. M. P. *Chem. Soc. Rev.* **1995**, 329.

(7) (a) Braga, D.; Grepioni, F.; Sabatino, P.; Desiraju, G. R. *Organometallics* **1994**, *13*, 3532. (b) Biradha, K.; Desiraju, G. R.; Braga, D.; Grepioni, F. *Organometallics* **1996**, *15*, 1284.

(8) Braga, D.; Biradha, K.; Grepioni, F.; Pedireddi, V. R.; Desiraju, G. R. *J. Am. Chem. Soc.* **1995**, *117*, 3156. Braga, D.; Grepioni, F. *Acc. Chem. Res.* **1997**, *30*, 81.

(9) Braga, D.; Grepioni, F.; Tedesco, E.; Desiraju, G. R.; Biradha, K. *Organometallics* **1996**, *15*, 1284. Braga, D.; Grepioni, F.; Tedesco, E.; Desiraju, G. R.; Biradha, K. *Organometallics* **1997**, *16*, 1846.

(10) Jeffrey, G. A.; Saenger, W. *Hydrogen Bonding in Biological Structures*; Springer-Verlag: Berlin, 1991.

(11) Brock, C. P.; Duncan, L. L. *Chem. Mater.* **1994**, *6*, 1307.

(12) Allen, F. H.; Davies, J. E.; Galloy, J. J.; Johnson, O.; Kennard, O.; Macrae, C. F.; Watson, D. G. *J. Chem. Inf. Comput. Sci.* **1991**, *31*, 204.

Table 1. Crystal Data and Details of Measurements

	1	2	3	4	6a	6b	7
formula	C ₉ H ₁₆ O	C ₂₂ H ₄₀ O ₂	C ₁₂ H ₂₀ O	C ₁₂ H ₂₁ O ₃	C ₂₄ H ₄₀ O ₂ Pt	C ₂₄ H ₄₀ NiO ₂	C ₂₂ H ₃₆ O ₂ Pt
<i>M_r</i>	140.22	336.54	180.28	213.29	555.65	419.27	527.60
temp (K)	183(2)	183(2)	173(2)	183(2)	183(2)	183(2)	183(2)
cryst syst	triclinic	monoclinic	triclinic	triclinic	monoclinic	monoclinic	triclinic
space group	<i>P</i> $\bar{1}$	<i>C</i> 2/ <i>c</i>	<i>P</i> $\bar{1}$	<i>P</i> $\bar{1}$	<i>C</i> 2/ <i>c</i>	<i>C</i> 2/ <i>c</i>	<i>P</i> $\bar{1}$
<i>a</i> (Å)	6.151(1)	15.322(3)	9.425(3)	8.506(2)	15.739(5)	16.000(1)	10.001(1)
<i>b</i> (Å)	14.078(3)	11.641(2)	10.332(5)	8.836(2)	15.023(5)	14.892(1)	11.083(1)
<i>c</i> (Å)	17.565(4)	26.974(5)	12.061(4)	9.409(2)	41.998(9)	22.325(1)	11.123(1)
α (deg)	97.75(3)		91.25(3)	91.90(3)			66.04(1)
β (deg)	92.45(3)	105.54(1)	90.82(3)	112.38(3)			86.61(1)
γ (deg)	94.54(3)		95.70(3)	94.24(3)			77.60(1)
<i>V</i> (Å ³)	1500.2(5)	4635(2)	1168.2(8)	650.7(3)	9912(5)	4984.1(6)	1100.0(2)
<i>Z</i>	6	8	4	3	16	8	2
<i>F</i> (000)	468	1054	400	234	4448	1824	524
<i>D</i> _{calcd} (g cm ⁻³)	0.931	0.964	1.025	1.089	1.489	0.792	1.593
θ range (deg)	3–26	2–23	3–25	2–25	2–27.5	2–26	2–27.5
octants explored (<i>h</i> _{min} – <i>h</i> _{max} , <i>k</i> _{min} – <i>k</i> _{max} , <i>l</i> _{min} – <i>l</i> _{max})	0 to 7, –17 to 15, –20 to 21	–16 to 15, –12 to 0, –29 to 0	–11 to 11, –12 to 12, 0 to 14	–10 to 9, –10 to 10, 0 to 8	–20 to 19, 0 to 19, –54 to 0	0 to 19, –18 to 0, –27 to 25	–12 to 12, –12 to 13, 0 to 13
no. of measd rflns	5542	3000	3935	2133	10681	4915	4625
no. of unique rflns used in refinement	5060	2927	3709	1979	10506	4735	4394
no. of refined params	321	241	248	204	482	245	249
GOF on <i>F</i> ²	1.050	1.107	1.085	0.993	1.009	1.005	1.122
<i>R</i> ₁ (on <i>F</i> , <i>I</i> > 2s(<i>I</i>))	0.0555	0.0468	0.0544	0.0374	0.1021	0.0625	0.0491
<i>wR</i> ₂ (on <i>F</i> ² , all data)	0.3931	0.1469	0.1550	0.1111	0.2728	0.1919	0.1651

for C₂₂H₃₆O₂Pt (527.16): C, 50.08; H, 6.88. Found: C, 50.26; H, 6.87. IR (Nujol): $\tilde{\nu}$ = 1887 (s, C≡C); 3370 (s, OH) cm⁻¹. ¹H NMR (THF-*d*₆, 25 °C, 200 MHz): δ 1.28 (s, CH₃, 18 H), 1.67–1.97 (m, CH₂, 16 H), 3.77 (s, OH, 2 H). ¹³C NMR (THF-*d*₆, 25 °C, 50.3 MHz): δ 24.5, 43.5 (CH₂), 29.7 (CMe₃), 31.8 (CH₃), 75.3 (C–OH), 127.0, 132.1 (C≡). MS (EI): *m/e* 527 (M⁺, 14), the isotopic pattern corresponds well with the simulated one, 434 (M⁺ – H₂O – C(CH₃)₃, 26), 41 (100). Mp: 73 °C (dec at 240 °C).

Crystallization of Alkynes. 1,1-Dimethyl-3-*tert*-butylprop-2-yn-1-ol (**1**): slow sublimation at room temperature. 1,1-Diethyl-3-*tert*-butylprop-2-yn-1-ol (**2**): recrystallization from pentane, –78 °C. 1-Cyclohexyl-3-*tert*-butylprop-2-yn-1-ol (**3**): recrystallization from pentane, –25 °C. 1,1,4,4-Tetramethylbut-2-yne-1,4-diol (**4**): recrystallization from THF at room temperature.

X-ray Diffraction Data:¹⁴ X-ray measurements were made on a CAD4 diffractometer equipped with a graphite monochromator (Mo K α radiation, λ = 0.710 73 Å). The crystals were mounted in a cold nitrogen stream at 183 K. Data sets were collected at 183 K (173 K in the case of compound **3**) and corrected for Lorentz and polarization effects. Data for the platinum complexes **6a** and **7** were corrected for absorption by azimuthal scanning of high- χ reflections (max and min transmission 0.99 and 0.76 and 0.89 and 0.43 for **6a** and **7**, respectively).^{14a} The structures were solved by direct methods (SHELXS^{14b}) and refined by full-matrix least-squares techniques against *F*² (SHELXL93^{14c}). For compounds **1–4**, the hydroxyl hydrogen atoms were located by difference Fourier synthesis and refined isotropically (not refined in the case of **3**). This was not the case for **6a**, **6b**, and **7**; because of the uncertainty on the orientation of the O–H groups, no modeling was attempted and the hydrogen bond analysis has been confined to donor–acceptor distances. All (C)H hydrogen atoms were added in calculated positions and refined 'riding' on their respective carbon atoms. All non-hydrogen atoms were refined anisotropically. The tertiary butyl group is disordered in all three independent molecules of **1** (disorder 50:50), in one of the independent molecules of **3** (main image: minor image 73:27), and in one of the two ligands in **7** (main image:minor image 66:34). The unit cells of crystals **6a** and

6b are apparently related by doubling of the *c*-axis. Although the metal and the oxygen atoms occupy nearly the same relative position in space, this is not so for the other atoms. The difference in the molecular dimensions is sufficient to generate a slightly different packing arrangement and to cause doubling of the cell axis. It is also noteworthy that crystals **1**, **3**, **4**, and **6a** have more than one crystallographically independent molecule in the asymmetric units. All of these molecules have very similar molecular structures, and the differences will not be discussed. The presence of several independent molecules in the asymmetric unit is a fairly common phenomenon in crystals of alcohols.¹¹ Crystal data and details of measurement are reported in Table 1.

CSD Searches. Data were retrieved from the October 1996 updated version of the CSD for all crystal structures with an exact match between chemical and crystallographic connectivity. Only entries presenting atomic coordinates were considered. Crystal structures retrieved from CSD are identified by their respective REFCODES. Unless stated otherwise, all structural parameters are calculated on the basis of X–H distances normalized to the corresponding neutron diffraction values. All relevant crystal structures were selected from the search outputs and investigated by computer graphics.¹⁵ The computer program PLATON¹⁶ was used to analyze the metrical features of the hydrogen-bonding patterns.

Results and Discussion

Molecular Structures in the Solid State. Before proceeding with the discussion of the molecular organization and hydrogen bonding, we need to illustrate some structural features of the new alcohols and prop-2-yn-1-ol complexes discussed in this study. Important bond lengths and angles for 1,1-dimethyl-3-*tert*-butylprop-2-yn-1-ol (**1**), 1,1-diethyl-3-*tert*-butylprop-2-yn-1-ol (**2**), 1-cyclohexyl-3-*tert*-butylprop-2-yn-1-ol (**3**), 1,1,4,4-tetramethylbut-2-yne-1,4-diol (**4**), as well as for bis(1-cyclohexyl-3-*tert*-butylprop-2-yn-1-ol)Pt(0) (**6a**) and -Ni(0) (**6b**) and the bis(1-cyclopentyl-3-*tert*-butylprop-2-yn-1-ol)Pt(0) (**7**) are reported in Table 2.

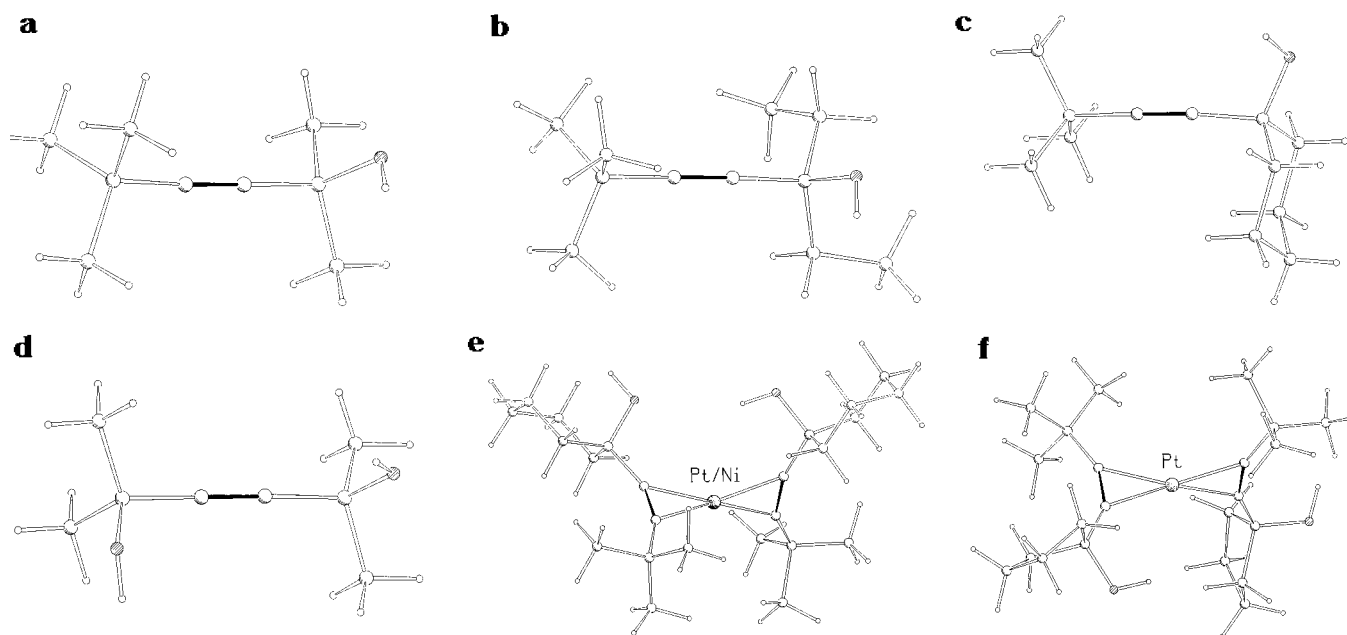
(14) (a) MOLEN, *An Interactive Structure Solution Procedure*; Enraf-Nonius: Delft, The Netherlands, 1990. (b) Sheldrick, G. M. SHELXS. *Acta Crystallogr., Sect. A* **1990**, *46*, 467. (c) Sheldrick, G. M. SHELXL93; University of Göttingen, Göttingen, Germany, 1993.

(15) Keller, E. SCHAKAL92, *Graphical Representation of Molecular Models*; University of Freiburg: Freiburg, Germany, 1992.

(16) Spek, A. L. PLATON. *Acta Crystallogr.* **1990**, *A46*, C31.

Table 2. Relevant Molecular Structural Parameters for Compounds **1**, **2**, **3**, **4**, **6a**, **6b**, and **7**

	1	2	3	4	6a	6b	7
$C_{sp} \equiv C_{sp}$	1.194(4), 1.190(4), 1.189(4)	1.191(4), 1.186(4)	1.189(4), 1.186(3)	1.193(3), 1.191(3)	1.33(3), 1.28(3), 1.27(3), 1.34(3)	1.242(7), 1.244(8)	1.299(13), 1.287(13)
$O-C_{sp^3}$	1.473(3), 1.432(3), 1.437(3)	1.438(3), 1.441(3)	1.444(3), 1.433(3)	1.429(2) ^a , 1.415(2), 1.429(2)	1.44(3), 1.42(3), 1.42(3), 1.42(3)	1.447(6), 1.442(6)	1.449(9), 1.435(13)
$C_{sp}-C_{sp^3}$	1.484(4), 1.483(4), 1.477(4)	1.480(4), 1.486(4)	1.476(4), 1.483(3)	1.479(2) ^a , 1.479(2), 1.485(2)	1.47(3), 1.53(3), 1.47(3), 1.53(3)	1.476(8), 1.484(8)	1.469(11), 1.435(13)
$C_{sp}-C^{tBu}$	1.472(4), 1.477(4), 1.478(3)	1.472(4), 1.480(4)	1.475(4), 1.484(3)		1.48(3), 1.50(3), 1.48(3), 1.38(3)	1.489(8), 1.493(9)	1.479(12), 1.476(13)
$M-C_{sp}$					1.99(2), 2.01(2), 1.96(2), 2.00(2), 2.03(2), 2.02(2), 1.96(2), 2.01(2)	1.873(5), 1.868(5), 1.852(5), 1.869(6)	2.016(8), 2.025(8), 2.019(8), 2.016(8)
$C_{sp} \equiv C_{sp}-C_{sp^3}$	179.2(3), 176.8(3), 179.4(3)	178.0(3), 174.8(3)	175.6(3), 173.2(3)	176.4(2) ^a , 178.1(2), 179.8(2)	161(2), 152(2), 158(2), 154(2)	156.0(6), 155.1(6)	154.4(8), 150.0(9)
$C^{tBu}-C_{sp} \equiv C_{sp}$	177.2(3), 178.0(3), 178.3(3)	178.6(3), 178.5(3)	179.5(3), 177.2(3)		149(2), 158(2), 153(2), 154(3)	156.3(6), 157.0(8)	110.3(10), 110.6(10), 110.2(10), 112.4(9), 107.5(9), 107.4(8)
$O-C_{sp^3}-C_{sp}$	109.1(2), 109.2(2), 109.1(2)	108.9(2), 110.4(2)	110.4(3), 106.1(2)	109.5(1), 109.9(1)	108(2), 106(2), 108(2), 108(2)	109.4(4), 109.4(4)	111.0(7), 109.5(8)

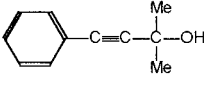
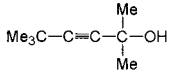
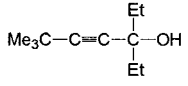
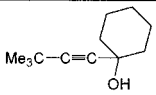
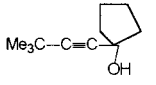
^a Molecule on an inversion center.**Figure 1.** Schematic representation of the molecular structures of (a) 1,1-dimethyl-3-*tert*-butylprop-2-yn-1-ol, **1**, (b) 1,1-diethyl-3-*tert*-butylprop-2-yn-1-ol, **2**, (c) 1-cyclohexyl-3-*tert*-butylprop-2-yn-1-ol, **3**, (d) 1,1,4,4-tetramethylbut-2-yne-1,4-diol, **4**, (e) bis(1-cyclohexyl-3-*tert*-butylprop-2-yn-1-ol)*M*(0) (*M* = Ni (**6a**), Pt (**6b**)), and (f) bis(1-cyclopentyl-3-*tert*-butylprop-2-yn-1-ol)Pt(0), **7**.

Sketches of all compounds are given in Figure 1. In both **1** and **3**, one of the *tert*-butyl groups is affected by rotational disorder around the $C_{sp}-C^{tBu}$ bond (see Experimental Section). For the sake of simplicity, the important structural parameters of the alcohols and complexes are discussed with reference to the $C^{tBu}-C_{sp} \equiv C_{sp}-C_{sp^3}$ backbone, *viz.* C_{sp} identifies the two carbon atoms of the alkyne, C^{tBu} the carbon atom of the *tert*-butyl group bound to C_{sp} , and C_{sp^3} the carbon atom carrying the $-OH$ group. In the case of **4**, which does not carry *tert*-butyl groups, the parameters are averaged over the two $C_{sp}-C_{sp^3}$ groups of the $C_{sp^3}-C_{sp} \equiv C_{sp}-C_{sp^3}$ system.

With respect to the data collected in Table 2, the following general comments can be made: (i) in all prop-

2-yn-1-ols the $C_{sp} \equiv C_{sp}-C_{sp^3}$ angles are very close to 180° , confirming that the prop-2-yn-1-ol system is rather stiff and not easily deformed by packing interactions; (ii) the $C_{sp} \equiv C_{sp}$ distance is, expectedly, longer in the complexes than in the "free" prop-2-yn-1-ols (this relationship is, however, less trustworthy in the case of **6a** because of the high esd's), and this lengthening upon coordination is accompanied by a substantial bending of the $C_{sp} \equiv C_{sp}-C$ angles from linearity to *ca.* 155° (see below for a discussion of these two effects); (iii) $C_{sp}-C_{sp^3}$ and $C^{tBu}-C_{sp}$ distances are strictly comparable as well as the $O-C_{sp^3}$ distance; (iv) in the complexes the $M-(C_{sp} \equiv C_{sp})$ interactions are symmetric, with shorter $M-C$ distances in the Ni complex than in the Pt ones.

Table 3. Comparison of Average Intermolecular O...O Distances (Å) in Prop-2-yn-1-ols and Their (Prop-2-yn-1-ol)₂Ni and Pt Complexes^a

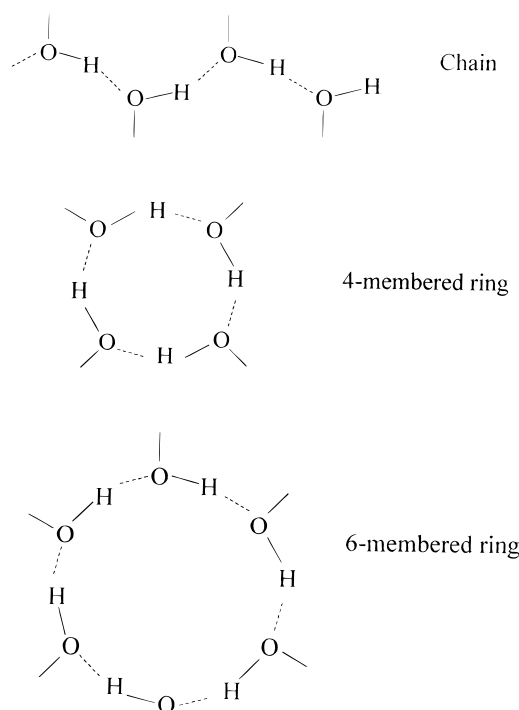
Alkynol / Ligand	Type of O-H...O pattern	O...O distance (Å) in free alkynols [REFCODE, ref.]	O...O distance (Å) in (alkynol) ₂ Ni complexes [ref.]	O...O distance (Å) in (alkynol) ₂ Pt complexes [ref.]
	chain	2.767(2) (mean) [FESMEV, 16]		
	chain	2.705(4) 2.706(4) 2.715(4) 1 [5]	2.777(3) 2.816(3) [5]	2.82(1) 2.83(1) [5]
	tetramer	2.749(3) 2.791(3) 2 [5]	2.788(4) 2.807(5) [5]	
	tetramer	2.768(3) 2.782(3) 3	2.865(6) 2.890(6) 6b	2.86(3) 2.89(3) 6a
	chain			2.81(1) 2.80(1) 7

^a When the reference is not specified, the reference is to this paper.

Hydrogen Bonding and Crystal Architecture in Alkynol Crystals and Comparison with Alkynol Complexes. Alkyne Monoalcohols and Alkyne Monoalcohol Complexes. Relevant information on the crystal structures of the monoalcohols and monoalcohol complexes discussed in this paper are reported in Table 3. The compound (C₆H₅)C≡C(CMe₂OH)¹⁷ (FESMEV) has been extracted from the CSD. Intermolecular O...O separations are given together with a description of the type of hydrogen-bonding pattern.

Intermolecular hydrogen bonding patterns have been discussed in detail by Brock and Duncan.¹¹ With few exceptions, alcohol molecules form one of the three packing patterns shown in Chart 1. These are the chain and the four- and the six-membered ring, identified by the notations C₂, R₄⁴(8), and R₆⁶(12) in graph set notation.¹⁸ Some compounds also form dimers (D). In simple monoalcohols, rings and chains have been shown to be equally probable; among the ring systems, however, tetramers are about three times as probable as the hexamers. About half of the chains have been shown to be either strictly or approximately helical. The average O...O distance in monoalcohols is 2.79(1) Å, the range being 2.55–3.05 Å.

1,1-Dimethyl-3-*tert*-butylprop-2-yn-1-ol forms chains as shown in Figure 2a, whereas 1,1-diethyl-3-*tert*-butylprop-2-yn-1-ol, and 1-cyclohexyl-3-*tert*-butylprop-2-yn-1-ol form tetramers as shown in Figures 2b and 2c, respectively. In terms of O...O distances, it can be

Chart 1

observed that the chain motif allows the shortest bonds to be formed (2.705(4), 2.706(4), 2.715(4) Å) while O...O lengths increase on moving to the tetramers, with intermediate distances shown by the diethyl alcohol (2.749(3), 2.791(3) Å) and slightly longer values shown by the cyclohexyl alcohol (2.768(3), 2.782(3) Å).

(17) Singelenberg, F. A. J.; van Eijck, B. P. *Acta Crystallogr.* **1987**, C43, 693.

(18) Bernstein, J.; Davis, R. E.; Shimoni, L.; Chang, N.-L. *Angew. Chem., Int. Ed. Engl.* **1995**, 34, 1555.

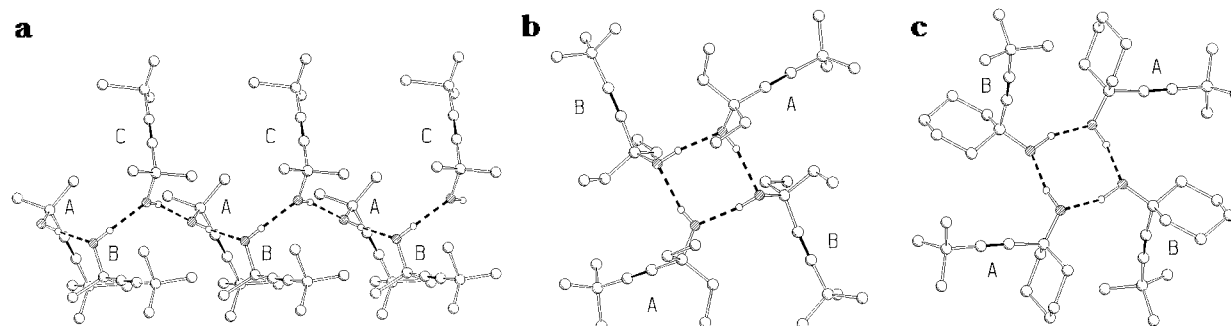


Figure 2. Molecular architecture in the solid state: (a) the chain formed by O—H...O interactions involving the three independent molecules in 1,1-dimethyl-3-*tert*-butylprop-2-yn-1-ol, **1** and the (OH)₄ tetramer involving both of the independent molecules in (b) 1,1-diethyl-3-*tert*-butylprop-2-yn-1-ol, **2**, and (c) 1-cyclohexyl-3-*tert*-butylprop-2-yn-1-ol, **3**. The disorder of the *tert*-butyl groups in **1** is not shown for clarity. Dashed atoms represent the O atoms. (C)H atoms have been removed for clarity.

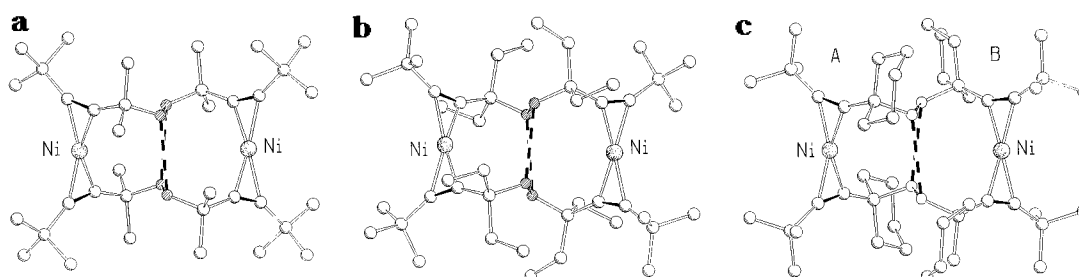


Figure 3. Hydrogen-bonded 'dimers' in (a) dimethyl, (b) diethyl, and (c) cyclohexyl *tert*-butylprop-2-yn-1-ol complexes of nickel. Note that in spite of the different complexity and geometry of the ligands, in all cases the geometry of the resulting (OH)₄ tetramer is that of a slightly distorted square.

Table 4. Intermolecular Hydrogen-Bond Pattern and Distances for Free Diols and Diol Complexes

REFCODE	compound	type of pattern	mean O...O distance (Å)	ref
DMHXDL01	HOEt ₂ C—(CH ₂) ₂ —CMe ₂ OH	connected polymer chains	2.72	20, 21
DMHXDM	<i>trans</i> -HOEt ₂ C—CH=CH—CMe ₂ OH	tetrahedrons	2.76	22
4	HOEt ₂ C—C≡C—CMe ₂ OH	six-membered rings	2.72(1)	<i>a</i>
	(HOEt ₂ C—C≡C—CMe ₂ OH) ₂ Ni	four-membered rings	2.76(3)	5e
	(HOEt ₂ C—C≡C—CMe ₂ OH) ₂ Pt	four-membered rings	2.73(3)	5a
	(HOEt ₂ C—C≡C—CET ₂ OH) ₂ Ni	four-membered rings	2.92(2)	5e
EOCYPT	(HOEt ₂ C—C≡C—CET ₂ OH) ₂ Pt	four-membered rings	2.95(3)	5f

^a This paper.

These patterns and relative geometrical parameters ought to be compared with those established by the corresponding bis(prop-2-yn-1-ol) complexes. As shown in Table 3, O...O separations increase markedly on passing from free prop-2-yn-1-ols to η^2 -coordinated prop-2-yn-1-ols. In terms of packing patterns, we observe that, with the exception of the cyclopentyl derivative (see below), all monoalcohol derivatives form "dimers" in the solid state *via* O—H...O hydrogen bonds. The geometry of the aggregates in the case of nickel is shown in Figure 3. The Pt complexes, though differing slightly in O...O distances, are all isostructural with the nickel ones. The tetrameric arrangements of the —OH groups are adopted irrespective of the alcohol complexity and of the type of metal and are strictly comparable, in terms of geometry, with those formed by organic alcohols. The effect of complexation is manifested in an appreciable lengthening of the O...O separations (see Table 3). The increase of the steric requirements of the residue on the carbon carrying the —OH group also appears to cause lengthening of the O...O bonds because O...O bond formation brings the lateral chains in close contact. This is particularly appreciable in the case of the cyclohexyl alcohol.

Interestingly the polymer-like chains which are formed

by 1,1-dimethyl-3-*tert*-butylprop-2-yn-1-ol (Figure 2a) are also found in compounds of the type (prop-2-yn-1-ol)₄Ni₃.^{5c-d}

The formation of dimeric units in the complexes *via* O—H...O bonds not only maximizes the O...O approach but also generates a 'protected' system where the hydrogen bonded ring is encapsulated within a sheath of carbon atoms. This latter phenomenon is also observed when the steric effect of the prop-2-yn-1-ol allows the introduction of three nickel atoms per four prop-2-yn-1-ols; in this case, the polymer-like chain of the 'free' prop-2-yn-1-ol is transferred to the structure of the corresponding [1,1-dimethyl-3-*tert*-butylprop-2-yn-1-ol]₄Ni₃ complex. On the whole, the structures formed by these prop-2-yn-1-ol complexes in the solid state can be regarded as van der Waals systems (i.e., the most polar part is segregated within the organic envelope), and the packing of the complexes reduces to that of larger van der Waals objects. A similar segregational effect of polar groups has been previously observed in the crystal structure of transition metal carbonyl cluster anions carrying halide ligands.¹⁹ The space-filling representation of the dimer formed by the 1-cyclohexyl-3-*tert*-butylprop-2-yn-1-ol ligands in com-

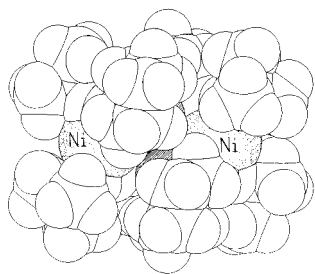


Figure 4. Space-filling representation of the hydrogen-bonded dimer in the nickel complex **6b**, showing how the hydrogen-bonded (OH)₄ frame is encapsulated within the 1-cyclohexyl-3-*tert*-butylprop-2-yn-1-ol ligands envelope.

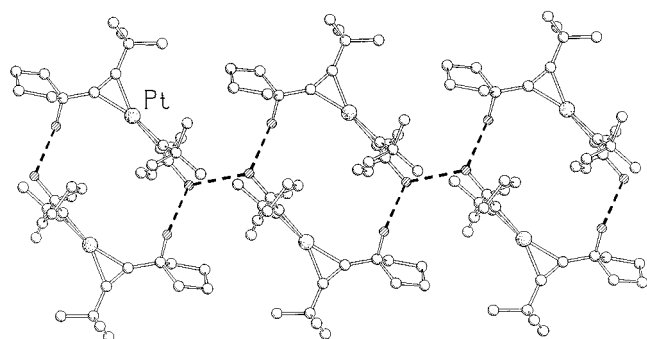


Figure 5. The chain-like system formed by the cyclopentyl *tert*-butyl prop-2-yn-1-ol Pt complex **7** along the *a*-axis. The *tert*-butyl disorder is not shown for clarity.

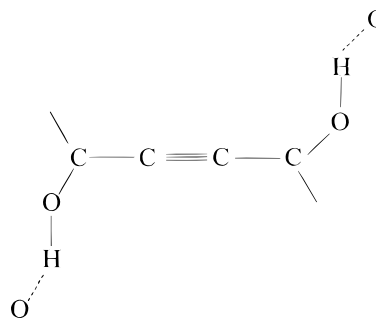
pound **6b** (Figure 4) shows how the entire (–OH)₄ unit is protected by the cyclohexyl groups.

As mentioned above, the cyclopentyl prop-2-yn-1-ol derivative is exceptional because the complexes do not form isolated 'dimers', as in the other cases, but form larger systems connected by O–H...O hydrogen bonds, which can be described as chains of dimers (see Figure 5). Each –OH group still participates in a one donor/acceptor interaction, the geometric difference arising from the orientation of one of the –OH groups, which are rotated by 109° with respect to the orientation observed in the other (prop-2-yn-1-ol)₂M complexes. The O...O distances are slightly shorter in the cyclopentyl than in the cyclohexyl derivative of Pt (2.80(1), 2.81(1) Å versus 2.87(3), 2.89(3) Å). Unfortunately, the structure of the corresponding organic alcohol is not, at yet, available.

Alkynediols and Alkynediol Complexes. Following the same conceptual path we can now move from alkyne monoalcohols to diols. Relevant structural information on some organic diols HOME₂C–C₂–CMe₂–OH is given in Table 4, together with CSD REFCODES and references to the original structural papers.

Organic alkynediols of the type HOR₂C–C≡C–CR₂–OH can have interesting applications in crystal engineering because of the presence of bidentate hydrogen bonding systems (the two –OH groups) separated by a stiff spacer in between (the triple bond). The hydrogen-bonding patterns reflect these characteristics: tetramers of the type observed with monoalcohols are no longer formed, and the resulting crystal architecture is based

Chart 2



either on chains (see Chart 2), as in crystalline HOME₂C–(CH₂)₂–CMe₂OH, or on ring systems, as in crystalline HOME₂C–C≡C–CMe₂OH. The crystal architecture generated by the alkynediol HOME₂–C≡C–CMe₂OH is illustrated in Figure 6a. The basic unit is a large hexameric system, formed via O–H...O bonds, in a chair-type conformation (see Figure 6b). In terms of O...O separations, this packing motif is comparable to those established by monoalcohols.

The dimethyl and diethyl alkyne derivatives of nickel and platinum show the same packing motif (see Figure 7). What was a dimer in the case of the corresponding *tert*-butyl monoalcohol now becomes a molecular row connected via two identical sets of hydrogen-bond rings on both sides of the metal centers. In spite of this similarity, however, there is a profound geometric change with respect to the bis(prop-2-yn-1-ol) complexes because the tetrameric O–H...O units are formed by two pairs of O–H groups belonging to the *same* ligand while they necessarily belong to the two different ligands in the bis(prop-2-yn-1-ol) complexes. Compared with the diol compounds in the bis(prop-2-yn-1-ol) complexes, the metal atom acts as an additional spacer between the OH groups of one donor/acceptor unit. This feature leads to a lengthening of the intraligand O...O distances in the bis(prop-2-yn-1-ol) complexes with respect to the bis(alkynediol) and causes a change in the conformation (from square/rhombus to butterfly) of the (OH)₄ rings.

The comparison between the tetramethyl alkynediol derivatives (see Table 4) shows that there is almost no effect on the hydrogen-bond systems if the nickel atom is replaced by the larger platinum atom. Average intermolecular O...O distances are 2.76₃ and 2.73₃ Å for the nickel and platinum complexes, respectively. On lengthening the aliphatic chains bound to the carbon atoms carrying the –OH groups, the structural effect is otherwise much more evident, although the packing motif based on joint tetrameric units is retained. In the case of the tetraethyl alkynediols, the intermolecular O...O distances average 2.92₂ and 2.95₃ Å for the nickel and platinum complexes, respectively.

The competition between formation of intermolecular bonds and that of intramolecular bonds needs also to be discussed. In the case of the cyclooctadiene derivative of the tetraethylalkynediol complex of nickel,⁷ for instance, the diol holds together a catemer-type molecular chain via a sequence of intramolecular and intermolecular O...O hydrogen bonds as shown in Figure 8. This is different from the packing motifs observed in both the monoalcohol and the bis(diols) complexes, which form dimers or rows of dimers. The most relevant structural difference between the two groups of complexes appears to be in the values of the C≡C–C angles

(19) (a) Braga, D.; Grepioni, F.; Milne, P.; Parisini, E. *J. Am. Chem. Soc.* **1993**, *115*, 5115. (b) Braga, D.; Grepioni, F.; Marshall, P.; Parisini, E. *Inorg. Chim. Acta* **1993**, *213*, 121. (c) Braga, D.; Grepioni, F.; Parisini, E. *J. Chem. Soc., Dalton Trans.* **1995**, 287.

(20) Helmholdt, B.; Reynars, H. *Acta Crystallogr.* **1976**, *B32*, 2243.

(21) Ulicky, L.; Kettmann, V. *Chem. Pap.* **1990**, *44*, 3.

(22) van der Wal, H.; Vos, A. *Acta Crystallogr.* **1990**, *B35*, 1730.

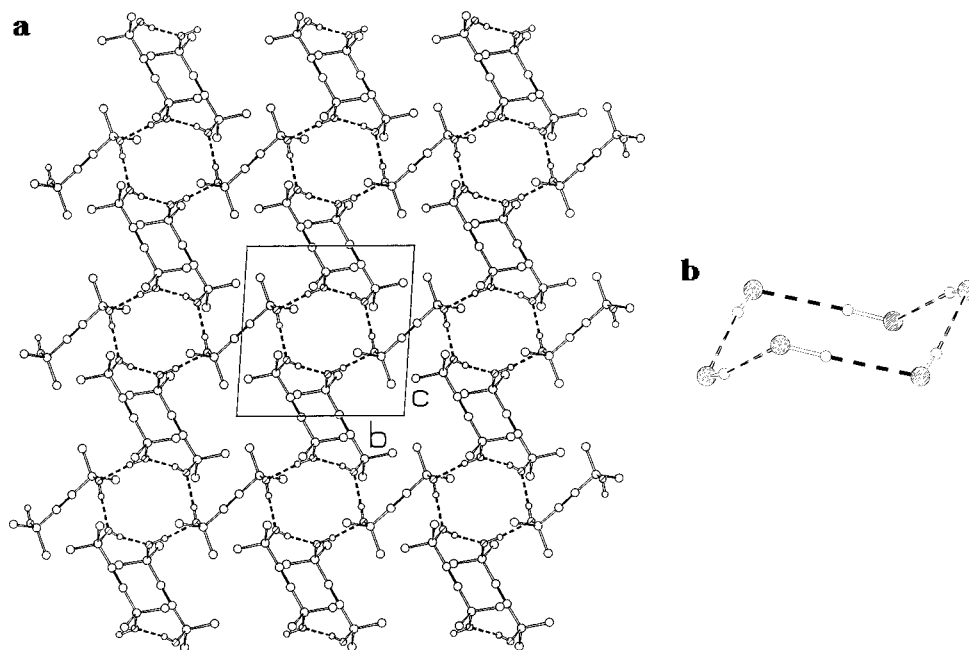


Figure 6. (a) View in the *bc*-plane of crystalline $\text{HOME}_2\text{C}-\text{C}\equiv\text{C}-\text{CMe}_2\text{OH}$, **4**, showing the hexameric systems formed *via* $\text{O}-\text{H}\cdots\text{O}$ bonds. (b) The chair-type conformation of the six-membered $(\text{OH})_6$ ring.

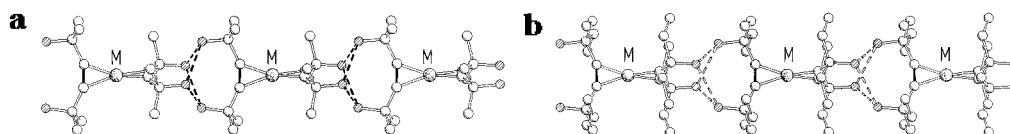


Figure 7. Molecular rows connected *via* hydrogen-bond rings on either side of the metal centers in the case of the (a) (dimethyl) and (b) (diethyl) alkynediol derivatives of nickel and platinum ($\text{M} = \text{Ni}, \text{Pt}$).

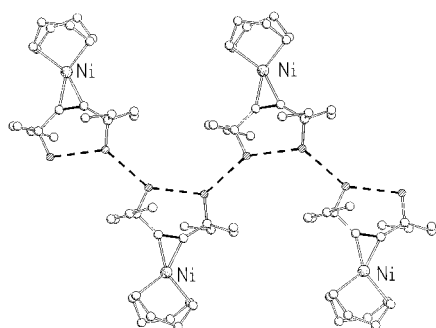


Figure 8. The catemer-type molecular chain along the *b*-axis in crystalline $(1,1,4,4\text{-tetraethylbut-2-yne-1,4-diol})\text{Ni}(\text{cod})$, formed by a sequence of intramolecular and intermolecular $\text{O}(\text{H})\cdots\text{O}$ hydrogen bonds.

which are larger in the bis(diol) complexes ($>150^\circ$) than in the monodiol complexes (ca. 140°). This also applies to the pair of molecules carrying the tetraethylidol ligand. A small value for the inner angle at the coordinated alkyne appears to be the condition for intramolecular hydrogen-bond formation.

Correlation with Raman/IR Stretching Frequencies. The geometric differences in compounds L_2Ni -(alkynediol) ($\text{L}_2 =$ bidentate or two monodentate ligands) correlate with alkyne triple bond strength, as reflected by Raman/IR stretching frequencies of the $\text{C}\equiv\text{C}$ bond. Intra- and intermolecular $\text{O}-\text{O}\cdots\text{O}$ hydrogen bond formation affects the $\text{C}\equiv\text{C}-\text{C}$ angle, hence the Raman/IR stretching frequencies can be used as a diagnostic tool for recognition of hydrogen bond formation and typology. $\Delta\tilde{\nu}$ values are calculated as the difference between the stretching frequency ($\tilde{\nu}$) of the free alkyne and that of the corresponding coordinated alkyne. Data

is grouped in Table 5. Compounds which show larger $\Delta\tilde{\nu}$ values, smaller $\text{C}\equiv\text{C}-\text{C}$ angles, and smaller intramolecular $\text{O}\cdots\text{O}$ distances form intramolecular hydrogen bonds. On the other hand, compounds which show smaller $\Delta\tilde{\nu}$ values, larger $\text{C}\equiv\text{C}-\text{C}$ angles, and larger intramolecular $\text{O}\cdots\text{O}$ distances form only intermolecular hydrogen bonds.

The same behavior has also been observed in several binuclear compounds of the formula $(1,2\text{-diamine})\text{Ni}(\mu\text{-alkynediol})\text{Ni}(\text{alkynediol})$ which contain bridging alkyne ligands and terminal alkyne ligands in the molecule.^{5e} The bridging alkynediols which show larger $\Delta\tilde{\nu}$ values, smaller $\text{C}\equiv\text{C}-\text{C}$ angles, and smaller $\text{O}\cdots\text{O}$ distances between the OH groups of the alkyne with respect to the terminally bound alkynediols form hydrogen bonds between these OH groups. On the other hand, the terminally bound alkynediols do not form intramolecular $\text{O}-\text{H}\cdots\text{O}$ bonds. A second point needs to be discussed. Substitution of the non-alkyne ligands *L* generates different hydrogen-bond patterns (as in compounds $\text{L}_2\text{Ni}(\text{HOCH}_2-\text{C}\equiv\text{C}-\text{CH}_2\text{OH})$ and $\text{L}_2\text{Ni}(\text{HOCMe}_2-\text{C}\equiv\text{C}-\text{CMe}_2\text{OH})$), whereas substitution of the alkyne ligands results in the same type of hydrogen-bond pattern (as in the cases of $\text{Ni}(\text{HOCHR}_2-\text{C}\equiv\text{C}-\text{CR}_2\text{OH})_2$ and $(\text{cod})\text{-Ni}(\text{HOCHR}_2-\text{C}\equiv\text{C}-\text{CR}_2\text{OH})$, respectively).

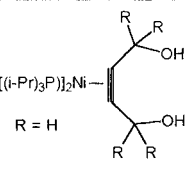
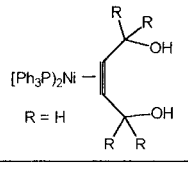
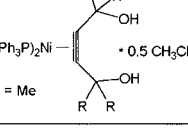
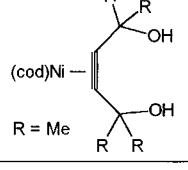
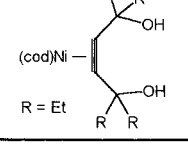
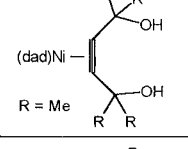
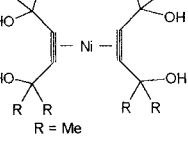
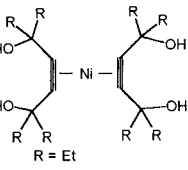
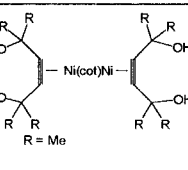
(23) Rosenthal, U.; Oehme, G.; Görls, H.; Burlakov, V. V.; Polyakov, A. V.; Yanovsky, A. I.; Struchkov, Yu. T. *J. Organomet. Chem.* **1991**, *409*, 299.

(24) Görls, H.; Schulz, B.; Rosenthal, U.; Schulz, W. *Cryst. Res. Technol.* **1988**, *23*, 25.

(25) Diercks, R.; Kopf, J.; tom Dieck, H. *Acta Crystallogr.* **1984**, *C40*, 363.

(26) Rosenthal, U.; Schulz, W.; Görls, H. *Z. Anorg. Allg. Chem.* **1987**, *550*, 169.

Table 5. Differences between the Raman/IR Stretching Frequency of the C≡C Bonds in Free Alkynes and in Their Nickel Complexes^a

REFCODE	compound	$\Delta\tilde{\nu}$ (C≡C) (cm ⁻¹)	angle C≡C-C (°)	O---O distance inside of the ligand (Å)	Presence of intramolecular hydrogen bonds	ref
KIYLIN	 R = H	431	138.5(3) 138.8(3)	2.81	yes	23
GIDHIK	 R = H	405	140.5(4) 142.1(5)	2.62	yes	24
LEWZOC	 R = Me • 0.5 CH ₃ CN	460	139.9(2) 142.2(2)	2.64	yes	6b
LEWZIW	 R = Me	423	144.5(6) 142.8(6)	2.57	yes	6b
	 R = Et	440	141.1 145.0	2.83	yes	6a
CELKIN	 R = Me	399	152.4(3) 152.4(3)	3.70	no	25
LEWZAO	 R = Me	341	156(1) 154(1) 158(1) 152(1)	3.67 3.71	no	6b
	 R = Et	344	155.3(1) 155.3(1) 155.3(1) 155.3(1)	3.73	no	6a
	 R = Me	379	151.5(4) 151.5(4) 151.5(4) 151.5(4)	6.00	no	6d

^a $\Delta\tilde{\nu} = \tilde{\nu}$ (free alkyne) - $\tilde{\nu}$ (coordinated alkyne), values for $\tilde{\nu}$ (C≡C): (a) for HOCH₂-C≡C-CCH₂OH = 2210 cm⁻¹, for HO-CMe₂-C≡C-CMe₂OH = 2230 cm⁻¹, given in ref 26; (b) for HO-CEt₂-C≡C-C-Et₂OH = 2248 cm⁻¹ (this work); dad = *N,N*-ethanediyldienbis(2,6-diisopropylaniline).

Conclusions

In this paper we have examined the crystal structures of organometallic complexes carrying prop-2-yn-1-ol ligands in comparison with those established by the corresponding organic alcohols. The stabilization afforded in the solid state by hydrogen bonds between alkynediol and prop-2-yn-1-ol groups in metal-coordinated alkynes has been exploited to isolate otherwise unstable, zerovalent homoleptic compounds. These complexes are of importance as starting materials for organometallic reactions and in catalytic processes.

Noncovalent intermolecular interactions established by organic and organometallic molecules both show many fundamental analogies but also several substantial differences. Clearly, the understanding of how noncovalent interactions can be tuned and controlled when metal atoms are involved represents a fundamental challenge. It may help to understand the mechanism of many homogeneous and heterogeneous catalytic processes as well as to develop some synthetic strategies in the field of supramolecular organometallic chemistry.

The main focus of this work has been on the patterns of intermolecular hydrogen-bonding interactions established in the solid state by prop-2-yn-1-ols and prop-2-yn-1-ol complexes. Structural information has been retrieved from the CSD or obtained specifically by determining the molecular and crystal structures of new prop-2-yn-1-ols and prop-2-yn-1-ol complexes. Some useful insight has been obtained. Indeed bis(prop-2-

yn-1-ol) complexes can be seen as *pseudo*-diols that dimerize and build (OH)₄ rings, as in the case of coordinated alkynediol molecules. The hydrogen-bonded network of the investigated free prop-2-yn-1-ols can be regarded as protected hydrogen-pattern systems, which can also take place in the corresponding metal compounds. In terms of the O...O distances, free alcohols form, in general, shorter hydrogen-bonded systems than the corresponding bis(alkyne) complexes. Although the ring appears to be the preferred packing motif in both organic and organometallic systems, on decreasing the bulkiness of the substituents chains or snakes are formed.

Acknowledgment. D.B. and F.G. acknowledge financial support by MURST and by the University of Bologna (Project: *Intelligent molecules and molecular aggregates*). D.B., F.G., D.W., and T.K. thank the Deutscher Akademischer Austauschdienst, Bonn, and the Conferenza Nazionale dei Rettori, Roma, for a scientific exchange grant within the Programme Vigoni.

Supporting Information Available: Tables of crystal data and structure refinement, anisotropic thermal parameters, fractional atomic coordinates, and bond lengths and angles and ORTEP diagrams with atomic labeling for **1–4**, **6a,b**, and **7** (53 pages). Ordering information is given on any current masthead page.

OM970331T